

Josephson junction in cobalt-doped BaFe₂As₂ epitaxial thin films on (La, Sr)(Al, Ta)O₃ bicrystal substrates

Takayoshi Katase^{a*}, Yoshihiro Ishimaru^b, Akira Tsukamoto^b, Hidenori Hiramatsu^c, Toshio Kamiya^a, Keiichi Tanabe^b and Hideo Hosono^{a,c}

a: Materials and Structures Laboratory, Mailbox R3-1, Tokyo Institute of Technology, 4259 Nagatsuta-cho, Midori-ku, Yokohama 226-8503, Japan

b: Superconductivity Research Laboratory, International Superconductivity Technology Center (ISTEC), 10-13 Shinonome 1-chome, Koto-ku, Tokyo 135-0062, Japan

c: Frontier Research Center, S2-6F East, Mailbox S2-13, Tokyo Institute of Technology, 4259 Nagatsuta-cho, Midori-ku, Yokohama 226-8503, Japan

ABSTRACT

Josephson junctions were fabricated in epitaxial films of cobalt-doped BaFe_2As_2 on [001]-tilt $(\text{La,Sr})(\text{Al,Ta})\text{O}_3$ bicrystal substrates. 10- μm -wide microbridges spanning a 30-degrees-tilted bicrystal grain boundary (BGB bridge) exhibited resistively-shunted-junction (RSJ)-like current–voltage characteristics up to 17 K, and the critical current was suppressed remarkably by a magnetic field. Microbridges without a BGB did not show the RSJ-like behavior, and their critical current densities were 20 times larger than those of BGB bridges, confirming BGB bridges display a Josephson effect originating from weakly-linked BGB.

Footnotes:

(*) Electronic mail: katase@lucid.msl.titech.ac.jp

The discovery of iron pnictide superconductors in early 2008¹ rekindled the extensive material research on superconductors.²⁻⁴ Materials in this new system possess attractive properties, including high critical temperatures (T_c) up to 56 K⁵ and high critical magnetic fields (upper critical fields > 100 T).^{6,7} These properties have aroused active research on epitaxial films and device applications of new high- T_c superconductors. Recently, we successfully fabricated epitaxial films of LaFeAsO⁸ and superconducting epitaxial films of cobalt-doped $A\text{Fe}_2\text{As}_2$ ($A = \text{Sr}$ and Ba) with T_c of ~ 20 K.^{9,10} Additionally, several groups have reported the fabrication of epitaxial films of Fe-based superconductors such as fluorine-doped LnFeAsO ($\text{Ln} = \text{La}, \text{Nd}$),¹¹⁻¹⁴ cobalt-doped $A\text{Fe}_2\text{As}_2$,¹⁵⁻¹⁹ and $\text{FeSe}_{1-x}\text{Te}_x$ ²⁰ with high $T_c \geq 20$ K. However, the crystal qualities, superconducting properties, and chemical stabilities must typically be improved to prepare superconducting devices. We initially tried to create a Josephson junction using cobalt-doped SrFe_2As_2 ($\text{SrFe}_2\text{As}_2:\text{Co}$) epitaxial films, but were unsuccessful due to the insufficient critical current density (J_c)²¹ and high reactivity even with water vapor in air.²² However, we later found that cobalt-doped BaFe_2As_2 ($\text{BaFe}_2\text{As}_2:\text{Co}$) epitaxial films are stable even in a moist atmosphere.¹⁰ In addition, $\text{BaFe}_2\text{As}_2:\text{Co}$ films exhibit an improved film quality compared to $\text{SrFe}_2\text{As}_2:\text{Co}$; e.g., $\text{BaFe}_2\text{As}_2:\text{Co}$ films have a better crystallinity and atomically-flat surfaces, although some droplets and pits defects remain.

Lee *et al.*¹⁵ fabricated bicrystal grain boundary (BGB) junctions in $\text{BaFe}_2\text{As}_2:\text{Co}$ epitaxial films on [001]-tilt SrTiO_3 (STO) bicrystal substrates, and reported the dependence of J_c on the misorientation angle of the BGB as well as the suppression of J_c across a BGB. Moreover, they reported growth of $\text{BaFe}_2\text{As}_2:\text{Co}$ epitaxial films and concluded that to obtain a high J_c of ~ 5 MA/cm² (at 4.2 K, self-field), a buffer layer

such as (001) STO and BaTiO₃ (BTO) is necessary for (La,Sr)(Al,Ta)O₃ (LSAT) substrates.¹⁸ Although the Josephson effect using a single-crystal of Fe-based superconductors has been reported,²³⁻²⁵ a Josephson junction based on epitaxial thin films, which is essential for practical device applications, has yet to be reported.

In this letter, we demonstrate a Josephson junction in an epitaxial film of a Fe-based superconductor. Distinct Josephson effects are observed in microbridges with BGB fabricated in BaFe₂As₂:Co epitaxial films grown on [001]-tilt LSAT bicrystal substrates.

BaFe₂As₂:Co epitaxial films (250 nm in thickness) were deposited on LSAT (001) single crystal and [001]-tilt LSAT bicrystal substrates with a 30-degree misorientation angle by pulsed laser deposition (PLD). The second harmonic of a Nd:YAG laser (wavelength: 532 nm) operating at a repetition rate of 10 Hz was used as the excitation source, and sintered disks of stoichiometric BaFe_{1.84}Co_{0.16}As₂ were employed as PLD targets. High quality epitaxial films were grown directly on LSAT (001) substrates without a buffer layer by the following process. In a previous paper,¹⁰ BaFe₂As₂:Co epitaxial films contained several % of Fe impurities and showed a superconducting transition width of $\Delta T_c = 3$ K and $J_c \ll 1$ MA/cm². Probably due to insufficient film quality, we could not obtain an operating Josephson junction with these films. Therefore, we improved the growth process to reduce the Fe impurity and to increase film uniformity, in particular by improving the phase purity of the PLD targets and the homogeneity of the substrate temperature. The PLD targets were synthesized by solid-state reactions of a stoichiometric mixture of BaAs, Fe₂As, and Co₂As via the reaction of $\text{BaAs} + 0.92\text{Fe}_2\text{As} + 0.08\text{Co}_2\text{As} \rightarrow \text{BaFe}_{1.84}\text{Co}_{0.16}\text{As}_2$. A key to obtaining a single-phase BaFe₂As₂:Co was to employ a finely-cut metal Ba reagent to complete the

reaction of the starting materials. In this work, we employed growth conditions at 850 °C and in a vacuum of $\sim 10^{-5}$ Pa.

Figure 1(a) shows the out-of-plane x-ray diffraction (XRD, anode radiation: $\text{Cu K}\alpha_1$) pattern of the improved $\text{BaFe}_2\text{As}_2\text{:Co}$ epitaxial film on a LSAT (001) substrate. Intense peaks of $\text{BaFe}_2\text{As}_2\text{:Co}$ $00l$ and LSAT $00l$ diffractions were observed, but peaks due to a metal Fe impurity, which should appear at $2\theta \sim 44$ and 65 degrees,¹⁰ were almost removed. Figure 1(b) shows the temperature dependence of the resistivity for the $\text{BaFe}_2\text{As}_2\text{:Co}$ films. Similar to those of single-crystals²⁶ and recently-reported epitaxial films,^{18,19} an onset transition temperature (T_c^{onset}) of ~ 22 K and a sharper transition temperature width (ΔT_c) of ~ 1.1 K were obtained. The film showed a high J_c of 2 – 10 MA/cm^2 at 3 K.

The BGB bridge structures were defined by photolithography and Ar ion milling. The BGB microbridge was 300- μm long and 10- μm wide. The I – V characteristics were measured by the four-probe method without and under magnetic fields perpendicular to the film. Figure 2(a) shows the in-plane ϕ scan of the 200 diffraction of a BGB bridge chip. Eight diffraction peaks, which were classified into two groups with a 90-degree rotational periodicity, were observed, confirming that the two crystals with the four-fold rotational symmetry coexist with a tilt angle of 30 degrees. This result verifies that the $\text{BaFe}_2\text{As}_2\text{:Co}$ BGB bridge has an epitaxial relationship with the LSAT bicrystal substrate. The resistivity measurements of the BGB bridge showed a sharp $\Delta T_c = 1.2$ K and $T_c^{\text{onset}} = 22.6$ K, both of which are the same as those obtained for the $\text{BaFe}_2\text{As}_2\text{:Co}$ epitaxial film in Fig. 1(b).

Figure 2(b) shows the current (I) – voltage (V) characteristics of the BGB bridge measured at 11 K, which exhibited a critical current (I_c) of 1.5 mA (J_c of 60 kA/cm^2)

without hysteresis. The shape of the $I - V$ curve indicates a resistively-shunted-junction (RSJ) type behavior at temperatures from 17 to 4.2 K. The estimated normal-state resistance R_N of the BGB bridge was $\sim 0.012 \Omega$, and the $R_N A$ product (A is the cross-sectional area of the junction) was $3.0 \times 10^{-10} \Omega \text{cm}^2$, which is smaller by an order of magnitude than that of a typical Josephson junction of a $\text{YBa}_2\text{Cu}_3\text{O}_{7-\delta}$ (YBCO) epitaxial film on a STO bicrystal substrate.²⁷ This result contrasts the case of a YBCO Josephson junction; i.e., it is considered that the low carrier density regions formed due to facets and a distorted lattice would result in a large R_N for the YBCO Josephson junction.²⁸ We tentatively attribute the small R_N of the $\text{BaFe}_2\text{As}_2:\text{Co}$ Josephson junction to the metallic nature of the normal state.

In contrast, the $I - V$ characteristics of microbridges without BGB (non-BGB bridge) did not show a RSJ-like behavior and only exhibited a resistivity jump due to the normal-state transition at J_c of $\sim 2 \text{ MA/cm}^2$ at 11 K. This result demonstrates that, even if the microbridge region contains domain/grain boundaries, a boundary with a small rotation mismatch does not work as a Josephson junction.

The uniformity of the current distribution across the junction was examined by measuring I_c of the BGB bridge as a function of the magnetic field (B) perpendicular to the film. The $I - V$ curves at $B = 0$ and $\sim 0.9 \text{ mT}$ in Fig. 3(a) demonstrate that I_c is clearly suppressed by applying a magnetic field at 10 K. The magnitude of I_c modulation, which is defined as $[I_c(0) - I_c(0.9 \text{ mT})] / I_c(0)$, was $\sim 95\%$, indicating that most of the supercurrent through the BGB bridge is due to the Josephson current. Figure 3(b) shows the $I_c - B$ pattern at 10 K. (The yellow arrow indicates the sweep direction.) The $I_c - B$ pattern showed a hysteresis, and the maximum I_c was observed at nonzero field values (e.g., at $\sim 0.7 \text{ mT}$ as indicated by the red triangle). The presence of hysteresis is

attributed to the influence of the flux pinnig in the vicinity of the BGB, similar to the case of BGB Josephson junctions using YBCO epitaxial films.²⁹ The $I_c - B$ curve did not show a clear multiple oscillation pattern and deviated from the ideal Fraunhofer pattern expected for a small junction with a uniform current distribution. Additionally, short-period oscillations, which are similar to a superconducting quantum interference device and attributed to nonuniform current flow across the junction due to inhomogeneous barriers and the existence of high resistance regions such as defects and dislocations, were observed. Considering the London penetration depth ($\lambda_L \sim 300$ nm) of BaFe₂As₂:Co at ~ 10 K,³⁰ the Josephson penetration depth λ_J was calculated by the following fomula, $\lambda_J = (\hbar / 2e\mu_0 d J_c)^{1/2}$ where d is the effective penetration depth $2\lambda_L$ ignoring barrier thicknesses, \hbar plank constant divided by 2π , e the elementary electric charge, and μ_0 the vacuum permeability. Using the observed J_c value of 88 kA/cm^2 gave a λ_J value of $1.8 \text{ }\mu\text{m}$, indicating that the junction is a “large junction” where the junction width ($10 \text{ }\mu\text{m}$) is much larger than λ_J . This suggests that the Josephson current flows in the edge regions of the junction.

Figure 4(a) shows the temperature dependece of J_c of the BGB bridge and a non-BGB bridge. The J_c of the BGB bridge is ~ 20 times smaller than that of the non-BGB bridge throughout the entire temperature range. For the BGB bridge, the supperconducting current was observed up to 18 K. Figure 4(b) shows the temperature dependence of the $I_c R_N$ product of the BGB bridge, which demosntrates that the value decreased almost linearly with increasing temperature. The inset is the $R_N - T$ plot. R_N almost remained unchanged at $T < 12$ K, which is the same behavior as the BGB Josephson junctions of YBCO epitaxial films.²⁷ R_N of the present system increased

gradually with increasing temperature at higher T . This dependence differs from that of the YBCO case where the R_N value is almost unchanged up to T_c .

In summary, we demonstrated Josephson junctions with 10 μm -wide microbridges across a bicrystal grain boundary in $\text{BaFe}_2\text{As}_2\text{:Co}$ epitaxial films on LSAT [001]-tilt bicrystal substrates. The $I - V$ curve displayed RSJ-like characteristics from 17 K to 4.2 K. The critical current was clearly modulated by an external magnetic field applied perpendicular to the film surface. We expect the present achievement will lead to the development of superconducting devices and circuits based on the epitaxial technology of Fe-based high- T_c superconductors.

This work conducted at the International Superconductivity Technology Center (ISTEC) was supported by New Energy and Industrial Technology Development Organization (NEDO), Japan. The present work was supported in part by the Funding Program for World-Leading Innovative R&D on Science and Technology, Japan.

References

1. Y. Kamihara, T. Watanabe, M. Hirano, and H. Hosono, *J. Am. Chem. Soc.* **130**, 3296 (2008).
2. M. Rotter, M. Tegel, and D. Johrendt, *Phys. Rev. Lett.* **101**, 107006 (2008).
3. X. C. Wang, Q. Q. Liu, Y. X. Lv, W. B. Gao, L. X. Yang, R. C. Yu, F. Y. Li, and C. Q. Jin, *Solid State Commun.* **148**, 538 (2008).
4. F. C. Hsu, J. Y. Luo, K. W. Yeh, T. K. Chen, T. W. Huang, P. M. Wu, Y. C. Lee, Y. L. Huang, Y. Y. Chu, D. C. Yan, and M. K. Wu, *Proc. Natl. Acad. Sci. USA* **105**, 14262 (2008).
5. C. Wang, L. Li, S. Chi, Z. Zhu, Z. Ren, Y. Li, Y. Wang, X. Lin, Y. Luo, S. Jiang, X.

- Xu, G. Cao, and Z. Xu, *Europhys. Lett.* **83**, 67006 (2008).
6. F. Hunte, J. Jaroszynski, A. Gurevich, D. C. Larbalestier, R. Jin, A. S. Sefat, M. A. McGuire, B. C. Sales, D. K. Christen, and D. Mandrus, *Nature* **453**, 903 (2008).
 7. H. Q. Yuan, J. Singleton, F. F. Balakirev, S. A. Baily, G. F. Chen, J. L. Luo, and N. L. Wang, *Nature* **457**, 565 (2009).
 8. H. Hiramatsu, T. Katase, T. Kamiya, M. Hirano, and H. Hosono, *Appl. Phys. Lett.* **93**, 162504 (2008).
 9. H. Hiramatsu, T. Katase, T. Kamiya, M. Hirano, and H. Hosono, *Appl. Phys. Express* **1**, 101702 (2008).
 10. T. Katase, H. Hiramatsu, H. Yanagi, T. Kamiya, M. Hirano, and H. Hosono, *Solid State Commun.* **149**, 2121 (2009).
 11. E. Backen, S. Haindl, T. Niemeier, R. Hühne, F. Freudenberg, J. Werner, G. Behr, L. Schultz, and B. Holzapfel, *Supercond. Sci. Technol.* **21**, 122001 (2008).
 12. T. Kawaguchi, H. Uemura, T. Ohno, R. Watanabe, M. Tabuchi, T. Ujihara, K. Takenaka, Y. Takeda and H. Ikuta, *Appl. Phys. Express* **2**, 093002 (2009).
 13. M. Kidszun, S. Haindl, E. Reich, J. Hänisch, L. Schultz, and B. Holzapfel, *Supercond. Sci. Technol.* **23**, 022002 (2010).
 14. S. Haindl, M. Kidszun, A. Kauffmann, K. Nenkov, N. Kozlova, J. Freudenberger, T. Thersleff, J. Werner, E. Reich, L. Schultz, and B. Holzapfel, *Phys. Rev. Lett.* **104**, 077001 (2010).
 15. S. Lee, J. Jiang, J. D. Weiss, C. M. Folkman, C. W. Bark, C. Tarantini, A. Xu, D. Abraimov, A. Polyanskii, C. T. Nelson, Y. Zhang, S. H. Baek, H. W. Jang, A. Yamamoto, F. Kametani, X. Q. Pan, E. E. Hellstrom, A. Gurevich, C. B. Eom, and D. C. Larbalestier, *Appl. Phys. Lett.* **95**, 212505 (2009).

16. E.-M. Choi, S.-G. Jung, N. H. Lee, Y.-S. Kwon, W. N. Kang, D. H. Kim, M.-H. Jung, S.-I. Lee, and L. Sun, *Appl. Phys. Lett.* **95**, 062507 (2009).
17. K. Iida, J. Hänisch, R. Hühne, F. Kurth, M. Kidszun, S. Haindl, J. Werner, L. Schultz, and B. Holzapfel, *Appl. Phys. Lett.* **95**, 192501 (2009).
18. S. Lee, J. Jiang, C. T. Nelson, C. W. Bark, J. D. Weiss, C. Tarantini, H. W. Jang, C. M. Folkman, S. H. Baek, A. Polyanskii, D. Abraimov, A. Yamamoto, Y. Zhang, X. Q. Pan, E. E. Hellstrom, D. C. Larbalestier, and C. B. Eom, "Template engineering of Co-doped BaFe₂As₂ single-crystal thin films," *Nat. Mater.* (to be published).
19. K. Iida, J. Haenisch, T. Thersleff, F. Kurth, M. Kidszun, S. Haindl, R. Huehne, L. Schultz, and B. Holzapfel, *Phys. Rev. B.* **81**, 100507 (2010).
20. E. Bellingeri, I. Pallecchi, R. Buzio, A. Gerbi, D. Marrè, M. R. Cimberle, M. Tropeano, M. Putti, A. Palenzona, and C. Ferdeghini, *Appl. Phys. Lett.* **96**, 102512 (2010).
21. B. Maiorov, S. A. Baily, Y. Kohama, H. Hiramatsu, L. Civale, M. Hirano, and H. Hosono, *Supercond. Sci. Technol.* **22**, 125011 (2009).
22. H. Hiramatsu, T. Katase, T. Kamiya, M. Hirano, and H. Hosono, *Phys. Rev. B* **80**, 052501 (2009).
23. X. H. Zhang, Y. S. Oh, Y. Liu, L. Q. Yan, K. H. Kim, R. L. Greene, and I. Takeuchi, *Phys. Rev. Lett.* **102**, 147002 (2009).
24. Y.-R. Zhou, Y.-R. Li, J.-W. Zuo, R.-Y. Liu, S. K. Su, G. F. Chen, J. L. Lu, N. L. Wang, and Y. -P. Wang, arXiv:0812.3295.
25. X. Zhang, S. R. Saha, N. P. Butch, K. Kirshenbaum, J. Paglione, R. L. Greene, Y. Liu, L. Yan, Y. S. Oh, K. H. Kim, and I. Takeuchi, *Appl. Phys. Lett.* **95**, 062510 (2009).

26. A. S. Sefat, R. Jin, M. A. McGuire, B. C. Sales, D. J. Singh, and D. Mandrus, *Phys. Rev. Lett.* **101**, 117004 (2008).
27. A. Odagawa, and Y. Enomoto, *Physica C* **252**, 141 (1995).
28. H. Hilgenkamp, J. Mannhart, and B. Mayer, *Phys Rev. B* **53**, 14586 (1996).
29. D. Dimos, P. Chaudhari, and J. Mannhart, *Phys. Rev. B* **41**, 4038 (1990).
30. R. T. Gordon, N. Ni, C. Martin, M. A. Tanatar, M. D. Vannette, H. Kim, G. D. Samolyuk, J. Schmalian, S. Nandi, A. Kreyssig, A. I. Goldman, J. Q. Yan, S. L. Bud'ko, P. C. Canfield, and R. Prozorov, *Phys. Rev. Lett.* **102**, 127004 (2009).

Figure captions

Fig. 1. (Color online) (a) out-of-plane XRD pattern at room temperature and (b) Temperature (T) dependence of electrical resistivity (ρ) of a $\text{BaFe}_2\text{As}_2\text{:Co}$ epitaxial film.

Fig. 2. (Color online) (a) In-plane ϕ scan of 200 diffractions of the BGB bridge on the LSAT bicrystal substrate at room temperature. (b) $I - V$ characteristic of the BGB bridge at $T = 11$ K.

Fig. 3. (Color online) (a) $I - V$ curves of the BGB bridge under $B = 0$ and 0.9 mT at $T = 10$ K. (b) Magnetic field dependence of the critical current (I_c) of the BGB bridge at 10 K. Yellow arrow and red triangle indicate the direction of the magnetic field sweep and the maximum I_c position, respectively.

Fig. 4. (Color online) (a) Temperature (T) dependences of critical current densities (J_c) of the microbridges with BGB ('BGB bridge') and without BGB ('non-BGB bridge'). (b) Critical current density – normal state resistance ($I_c R_N$) product as a function of temperature for the BGB bridge. Inset shows the temperature dependence of R_N .

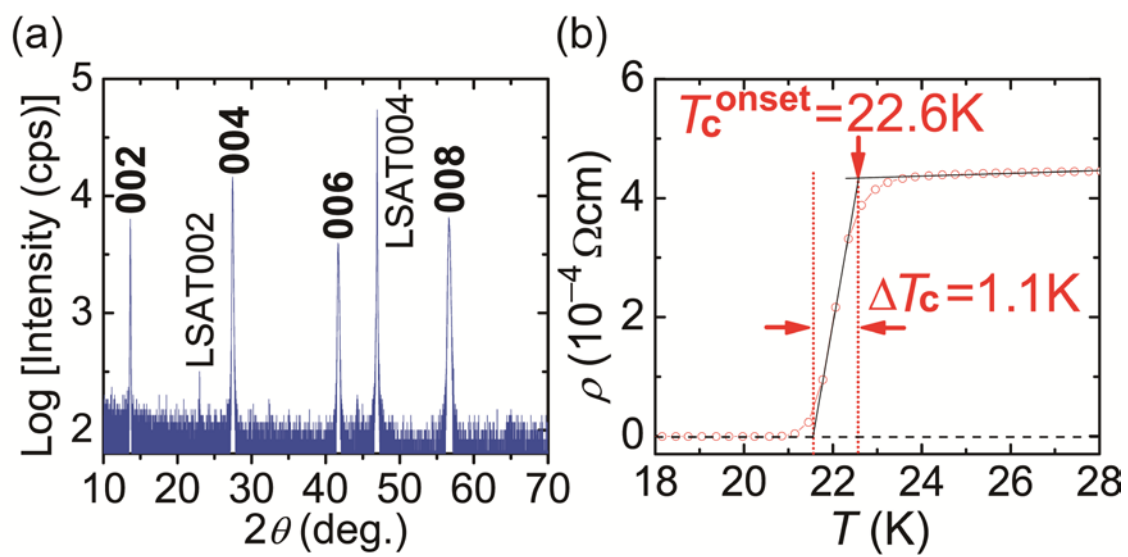


Fig. 1.

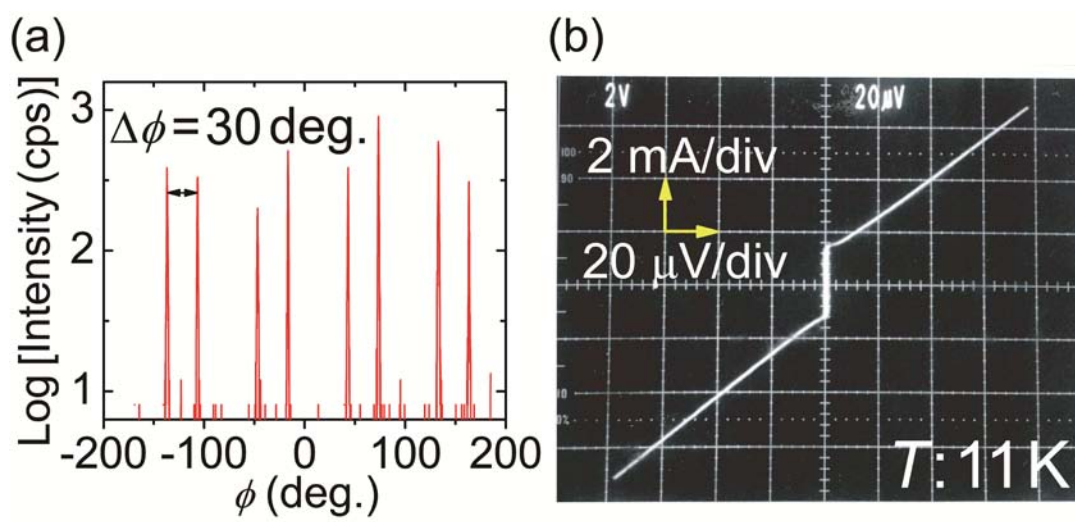


Fig. 2.

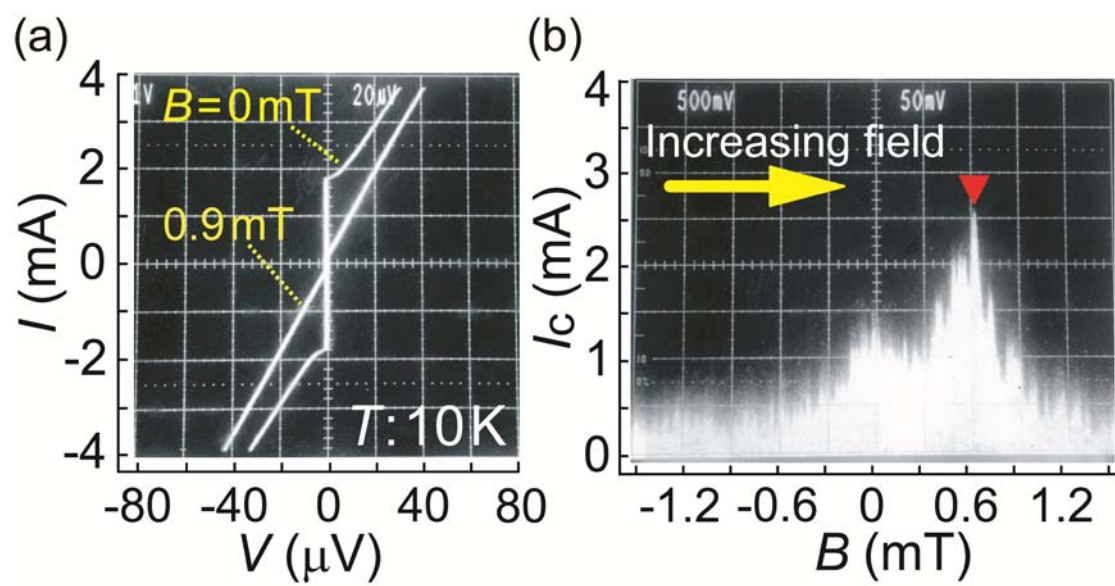


Fig. 3.

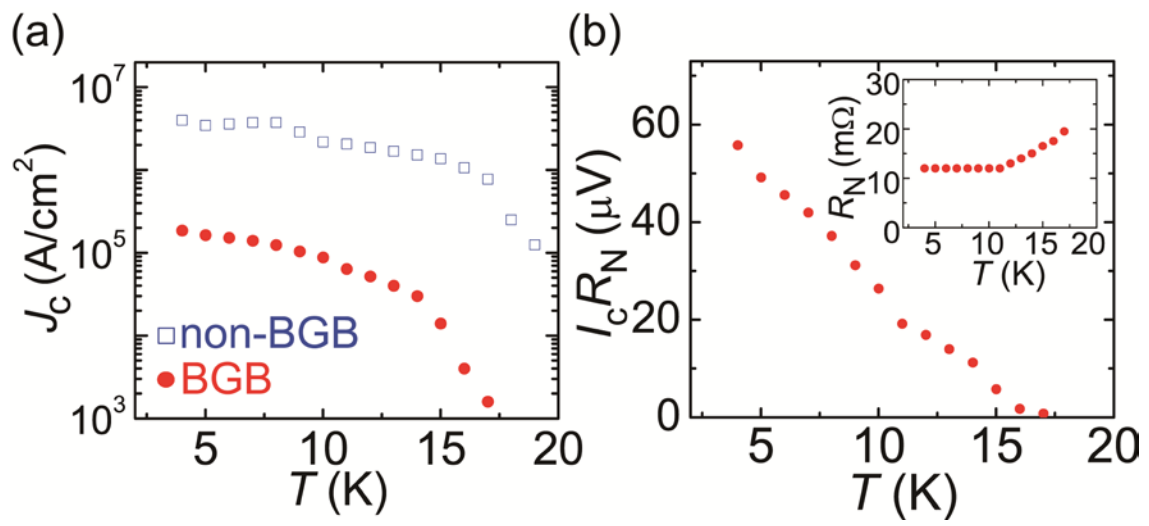


Fig. 4.

